Oligocene eustasy from two-dimensional sequence stratigraphic backstripping

Michelle A. Kominz*
Department of Geosciences, Western Michigan University, 1187 Rood Hall, Kalamazoo, Michigan 49008-5150, USA

Stephen F. Pekar
Lamont-Doherty Earth Observatory, Columbia University, Palisades, New York 10964-8000, USA

ABSTRACT

Estimates of the magnitudes of changes in third-order (0.5−2 m.y.) eustasy were obtained for Oligocene sequences defined by a suite of largely onshore boreholes of the New Jersey coastal plain. Benthic foraminiferal biofacies and multiple age constraints in a sequence stratigraphic framework formed the database for this study. The geometry of the margin through time was determined using two-dimensional backstripping. The depth ranges of benthic foraminiferal biofacies were determined from a combination of standard factor analysis techniques and the backstripped geometries. Benthic foraminiferal biofacies were then used to determine the depths of the Oligocene margin profiles obtained from backstripping. The water depths of 16 of these horizons were confirmed by independent benthic biofacies determinations from at least two wells. This internal consistency indicates that the data and the two-dimensional backstripping approach were robust. Where benthic biofacies require a vertical shift of the horizons generated by two-dimensional backstripping, eustatic changes were required and were readily calculated.

Results indicate a major eustatic fall from the end of the Eocene to the first record of Oligocene deposition. Subsequent long-term shoaling of sea level through the Oligocene was ~30 m in 10 m.y. Superimposed on this long-term trend were higher frequency (third-order) variations in eustasy with amplitudes of ~40 m or less.

*E-mail: michelle.kominz@wmich.edu.

Keywords: basin analysis, eustasy, New Jersey, Oligocene, sequence stratigraphy.

INTRODUCTION

One of the most critical and intractable problems in stratigraphy is the extraction of intertwined eustatic (global sea level) and tectonic signals. Despite attempts in the past few decades to separate the effects of tectonics from eustasy (e.g., Kominz et al., 1998; Sahagian and Jones, 1993; Reynolds et al., 1991; Watts and Steckler; 1979, Bond, 1979; Vail and Mitchum, 1977; Haq et al., 1987; Greenlee and Moore, 1988), significant problems remain (e.g., Christie-Blick and Driscoll, 1995; Christie-Blick, 1991; Steckler et al., 1999).

The extraction of these two signals from the stratigraphic record of transgressive and regressive facies is of considerable importance. A eustatic curve would make an outstanding chronostratigraphic tool (e.g., Haq et al., 1987). Knowing the part of any given stratigraphic record that is tectonic rather than eustatic would be instrumental in interpreting facies relations and in predicting the presence of source and/or reservoir horizons. The eustatic signal would provide an important reference

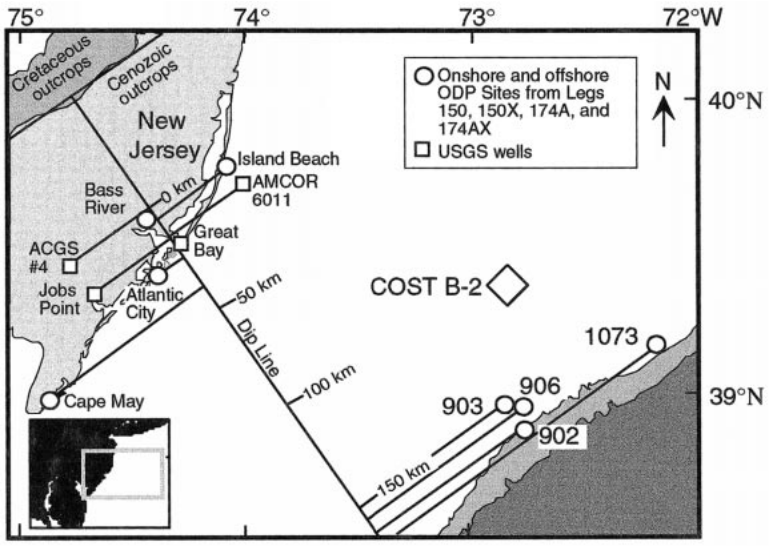

Figure 1. Southern part of New Jersey (see inset in lower left for larger view) with location of the sites used in this study: Leg 150 (Sites 902, 903, and 906); Leg 150X (Island Beach, Atlantic City, and Cape May boreholes); Leg 174A (Site 1073); and Leg 174AX (Bass River borehole). Also used in this study were U.S. Geological Survey onshore and offshore wells: AMCOR 6011, ACGS #4, Great Bay, and Jobs Point. Dip line is perpendicular to the Cretaceous outcrops, and strike lines were used to project from the wells onto the dip profile. The Cost B3 well was used to estimate compaction of sandstone and shale.

GSA Bulletin; March 2001; v. 113; no. 3; p. 291–304; 8 figures; 2 tables; Data Repository item 2001027.

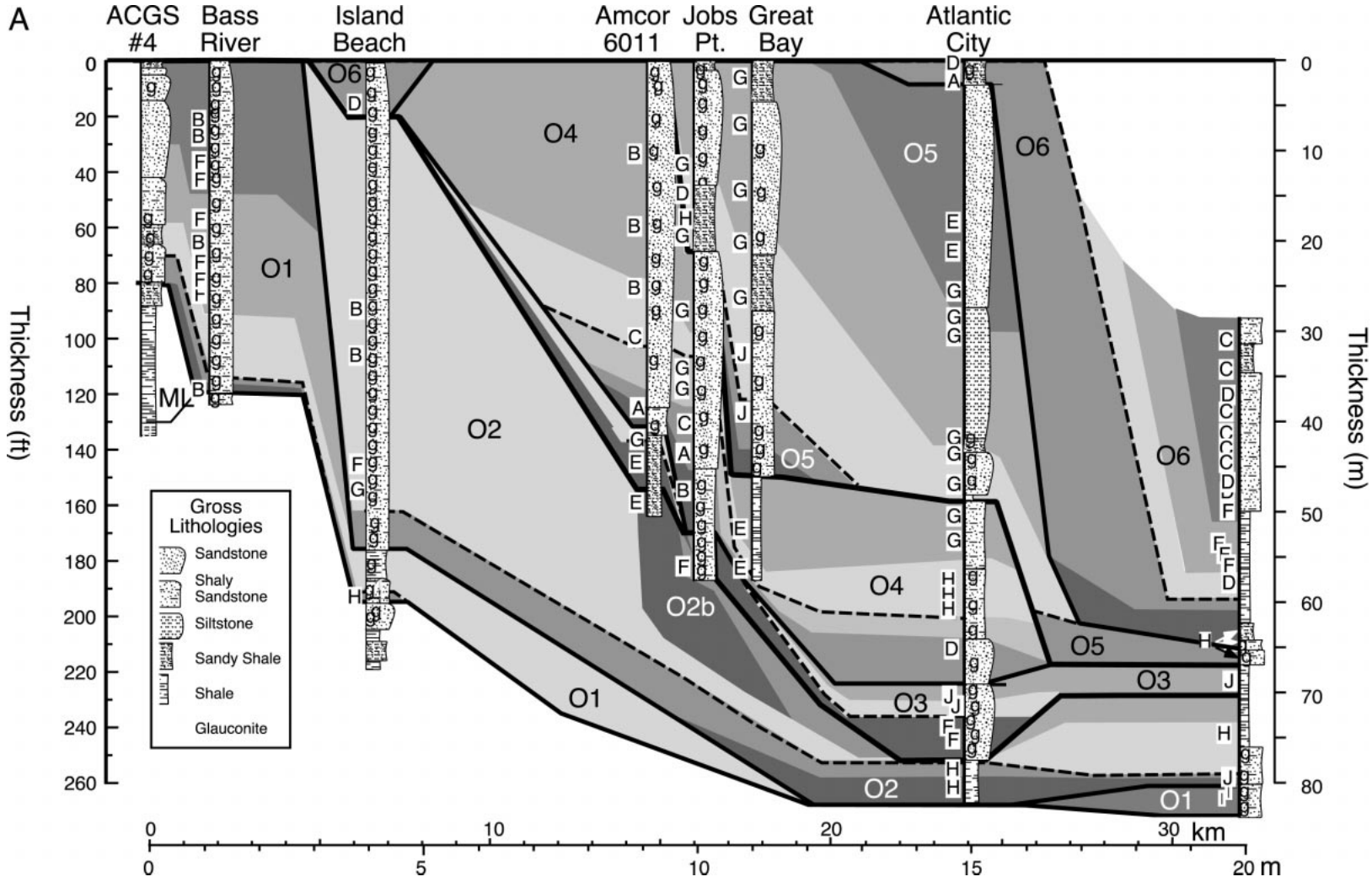

Figure 2. (A) Distribution of sequences used in this study. Sequence names are Mays Landing (ML) and Oligocene1 (O1) through Oligocene6 (O6). Observed thickness and gross lithologies are sketched for each borehole (see references in text for detailed lithology). The borehole data are hung from the top of the Oligocene, except the Cape May borehole, which consistently includes more distal, deeper water units. As such, its base is drawn roughly at the base of the Oligocene section in the adjacent Atlantic City borehole. Because the sediments are not decompacted, it is impossible to generate a realistic cross section. Borehole data are plotted according to their projected horizontal locations on the dip line shown in Figure 1. Uppercase letters to the left of each well give the locations of benthic foraminiferal biofacies, obtained by factor analysis and calibrated by application of two-dimensional backstripping (Pekar and Kominz, 2001). The deepest biofacies observed is designated by J; the shallowest is A (see Table 1). Thick lines connecting the wells are sequence boundaries; dashed lines are maximum flooding surfaces. Sediments below maximum flooding surfaces, transgressive deposits (Pekar et al., 1999), are depicted with dark to lighter grays, and those above (highstand deposits) are depicted by lightest to darker grays. Surfaces indicated by shading within systems tracts are generated by interpolation between dated intervals on each borehole (see B) (Pekar et al., 2000), and indicate the physical surfaces used in our analyses. (B) Chronostratigraphic chart for the New Jersey Oligocene sequence model (see 2A). Only the minimum and maximum age estimates (in millions of years) of each sequence in each well are shown. Error ranges for strontium isotope ages (Sr) were generally ±0.7 m.y. Multiple estimates at a single sample location often reduced this error range. The letter b beside the date indicates biostratigraphic age estimates. The letter M indicates magnetostratigraphic control. Where no uncertainty range is given, that age was extrapolated from data (not shown) within the sequence. Where no indication of the source of age control is given beside the date, it is based on a combination of these methods. Data shown here are from Pekar et al. (2000) and represent only a small subset of the age control.

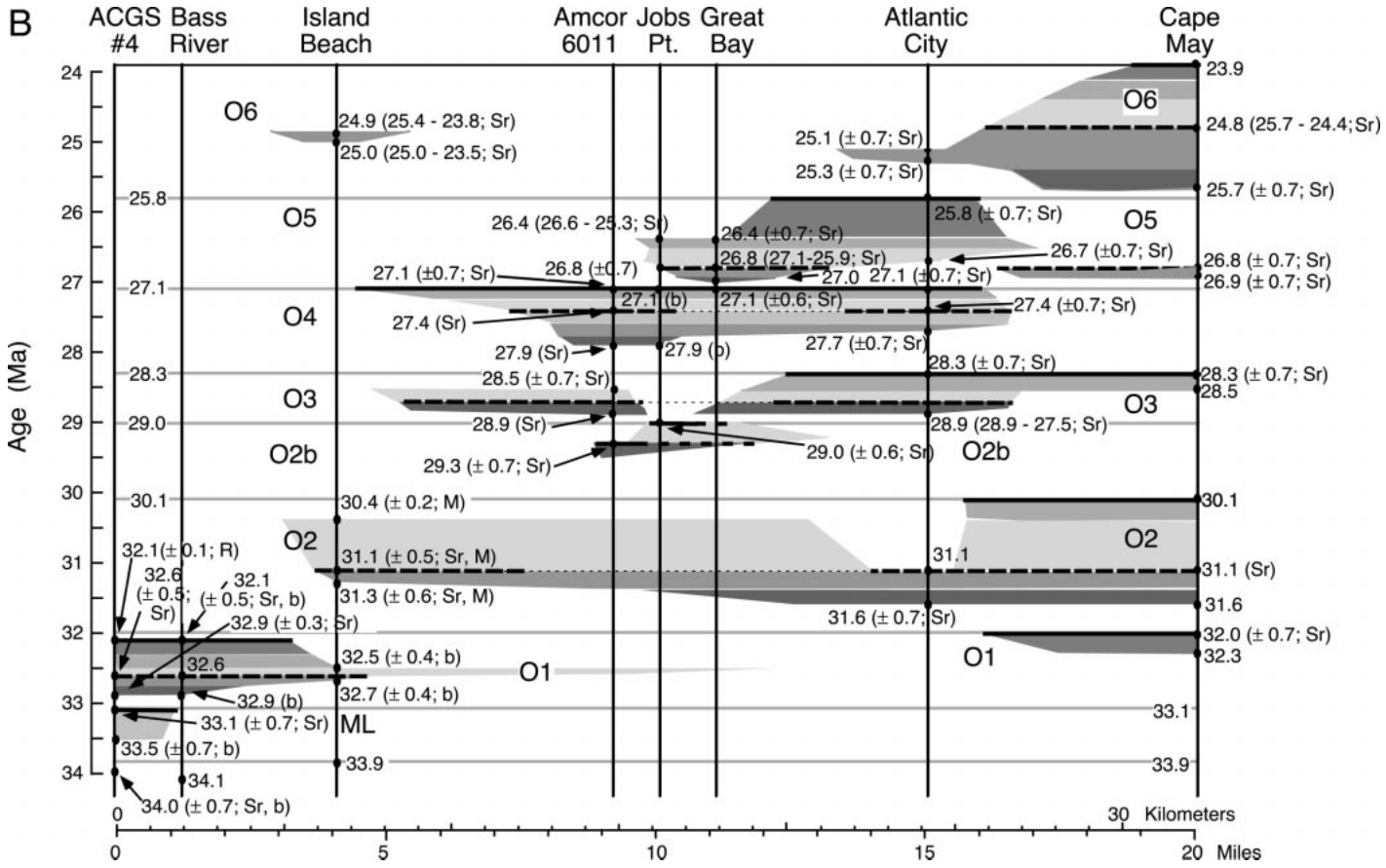

Figure 2. (*Continued.*)

against which to determine the tectonic signal in a complex tectonic regime. One of the outstanding questions of the past 20 yr is the source of third-order (duration of 0.5−2 m.y.) sea-level change. An important step in addressing this question is identifying the timing and magnitude of these events. A significant portion of this eustatic signal is often tied to continental ice sheets and climate (Miller and Fairbanks, 1985a; Miller et al., 1987, 1991). Knowing eustatic history would provide important clues to the Earth's climatic past (Miller et al., 1991; Zachos et al., 1992b).

In this paper we demonstrate that with a two-dimensional, sequence stratigraphic data set and detailed paleobathymetry in a thermally subsiding, tectonic regime, it is possible to extract the eustatic signal at the scale of 0.5 m.y. variations. Our data were from Oligocene strata of the New Jersey coastal plain with a tie to uppermost Eocene and to lowermost Miocene strata (34−23 Ma in the Berggren et al., 1995, time scale). The eustatic curve was not tied to present sea level but yields magnitudes of third-order sea-level change within the Oligocene, including the largest-magnitude sea-level fall of Haq et al. (1987).

DATABASE

The primary data for this work were obtained from boreholes drilled on the New Jersey coastal plain (Fig. 1), as a part of Ocean Drilling Program (ODP) Legs 150X and 174AX. These include the Cape May, Atlantic City, Island Beach, and Bass River boreholes, which were all continuously cored with good to excellent recovery (Pekar et al., 1997; Pekar, 1999). Additional samples used in this study came from: (1) the ACGS #4 borehole cores and cuttings (Poore and Bybell, 1988); (2) the discontinuously cored Jobs Point borehole (Olsson et al., 1980); (3) the continuously cored AMCOR 6011 borehole (Pekar, 1999; Pekar et al., 2000); and (4) the discontinuously cored Great Bay borehole (Pekar, 1999). Pekar et al. (1997) and Pekar (1999) gave detailed lithologic and chronostratigraphic descriptions of the Oligocene units (Data Repository Table DR1[1]).

[1]GSA Data Repository item 2001027, tables of input, output, and constraints on sea level, is available on the Web at http://www.geosociety.org/pubs/ft2001.htm. Requests may also be sent to Documents Secretary, GSA, P.O. Box 9140, Boulder, CO 80301; e-mail: editing@geosociety.org

ODP Sites 902, 903, 906 (Miller et al., 1996), and 1073 (Austin et al., 1998) were used to provide constraints on far-field flexural loading of the margin (Fig. 1; Table DR1). The data from the onshore and nearshore wells and boreholes were projected into a single, 32 km composite dip section, which was extended to 170 km to include the offshore well data (Fig. 1). The 32 km composite dip section suggests the presence of prograding clinoforms of Oligocene age (Fig. 2A), similar to those of Miocene age that have been imaged beneath the modern shelf (e.g., Poulsen et al., 1998; Fulthorpe and Austin, 1998; Greenlee and Moore, 1988). Recent high-resolution seismic imaging of the nearshore New Jersey margin revealed Oligocene clinoforms, corroborating this interpretation (Monteverde et al., 2000).

Ages assigned to the Oligocene sequences recognized in these wells were derived from a combination of Sr isotope chemostratigraphy, biostratigraphy, and magnetostratigraphy (Pekar et al., 2000; partially indicated in Fig. 2B). These data were combined within a sequence stratigraphic framework to estimate the ages of sequence boundaries and maximum flooding surfaces. While individual absolute age es-

timates yielded uncertainties of ±0.3 to ±0.7 m.y., the combined data set and sequence stratigraphic framework resulted in age estimates with a relative precision of about ±0.1 m.y. That is, within any given sequence, the relative stratigraphic correlation was considerably more precise than the absolute age uncertainty (Fig. 2B). As such, our results could be shifted, somewhat, to older or younger ages, requiring extension or compression in time. The magnitudes and relative positions (in time) of each sequence were not affected by this uncertainty.

Benthic foraminiferal biofacies were obtained by performing Q-mode factor analysis on samples from seven of the eight boreholes (uppercase letters in Fig. 2A). We extracted and rotated 10 principal components (eigenvalues >1) to maximize the variance explained by the data set (Varimax factor rotation; e.g., Lipps et al., 1979). As a result, 73.4% of the faunal variation was explained (Pekar and Kominz, 2001). The calibration of the biofacies to water depth was accomplished using the two-dimensional backstripping results. The calibration was critical to the sea-level estimates. Because of this, and to alleviate fears that the eustatic estimates are derived by circular reasoning, the calibration is discussed briefly in the following but is elaborated on in Pekar and Kominz (2001).

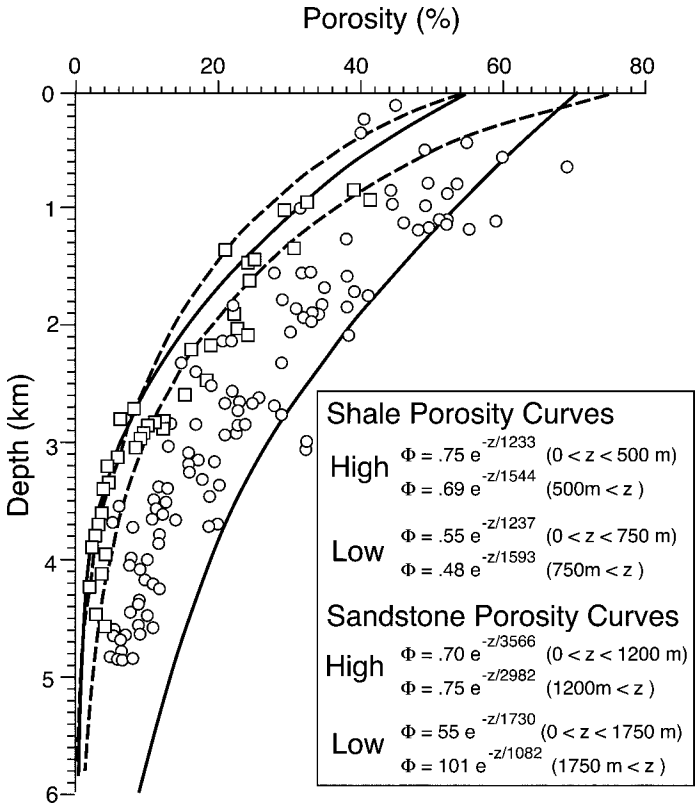

Figure 3. Sandstone and shale porosity vs. depth curves and equations used in the backstripping analyses compared to data from the Cost B3 well (Rhodehamel, 1977; Smith et al., 1976). Each bracketing set of porosity curves is composed of two exponential equations. Two sets of curves, high (maximum porosity vs. depth) and low (minimum porosity vs. depth), were used to estimate Oligocene surfaces and thus eustatic change. Circles represent sandstone and squares represent shale porosity observations.

BACKSTRIPPING PROCEDURE

Having established an age model with correlation between wells based on a sequence stratigraphic framework (Fig. 2; Pekar et al., 2000; Pekar 1999), the paleotopography of the Oligocene margin was reconstructed using a backstripping procedure similar to that of Steckler et al. (1999). The geometry of the Oligocene margin was determined by assuming the shape of the pre-Oligocene surface (discussed in the following) and estimating the subsidence of that surface through time and the thickness of Oligocene sediment, which was deposited on that surface. The pre-Oligocene (top of the Eocene) surface subsided through time as a result of compaction of the pre-Oligocene sediment, tectonic subsidence of the basement, and flexural loading by the Oligocene sediment. This procedure is dependent, in large part, on sediment thickness and density, obtained from one-dimensional backstripping. The input data used are presented in Table DR1 and described in the following. It is, however, fully independent of à priori Oligocene paleobathymetric estimates.

Data for backstripping the Cape May, Atlantic City, and Island Beach boreholes were presented in Kominz et al. (1998; GSA Data Repository item 9834). More detailed Oligocene data were used for backstripping the Island Beach borehole (Table DR1). These data are from Pekar and Miller (1996), Pekar et al. (1997, 2000), and Pekar (1999). The remainder of the wells and boreholes had not been previously backstripped.

The Bass River borehole data were from Miller et al. (1998a). Underlying sediment lithologies (pre−Bass River Formation) were taken from the Island Beach rotary core and reduced to the overall thickness estimated beneath the Bass River borehole (~420 m of the Potomac Formation, Table DR1).

Only Oligocene lithologic and age data were available from the Jobs Point, AMCOR 6011, and Great Bay boreholes (Table DR1; Pekar, 1999). We assumed that underlying and overlying sediment lithologies were identical to the nearby Island Beach borehole (Kominz et al., 1998). Thickness was increased in proportion to the distance between each well and the Island Beach borehole on the composite dip section. A similar procedure was used with the ACGS #4 borehole using sediment thickness in proportion to the Bass River borehole. Oligocene sediment lithology, age, and thickness (Table DR1) are from Pekar (1999). While these procedures are far from ideal, the relatively simple tectonic and depositional environment of the New Jersey coastal plain minimizes the impact of variations in the strata below the Oligocene.

ODP wells (Sites 902, 903, 906, and 1073, Fig. 1) were used in this analysis only to estimate the impact of offshore flexural loading during the Oligocene. As such, the overlying sediment thickness was required to remove the porosity from the Oligocene sediment packages. Oligocene sediment lithologies and ages of these wells (Table DR1) were from Pekar et al. (2000), Miller et al. (1996, 1998a), Pekar (1999), Olsson et al. (1980).

Sandstone, shale, and glauconite dominated the Oligocene sequences (Table DR1; Fig. 2A). Glauconite was assumed to compact in the same manner as sandstone. Porosity versus depth

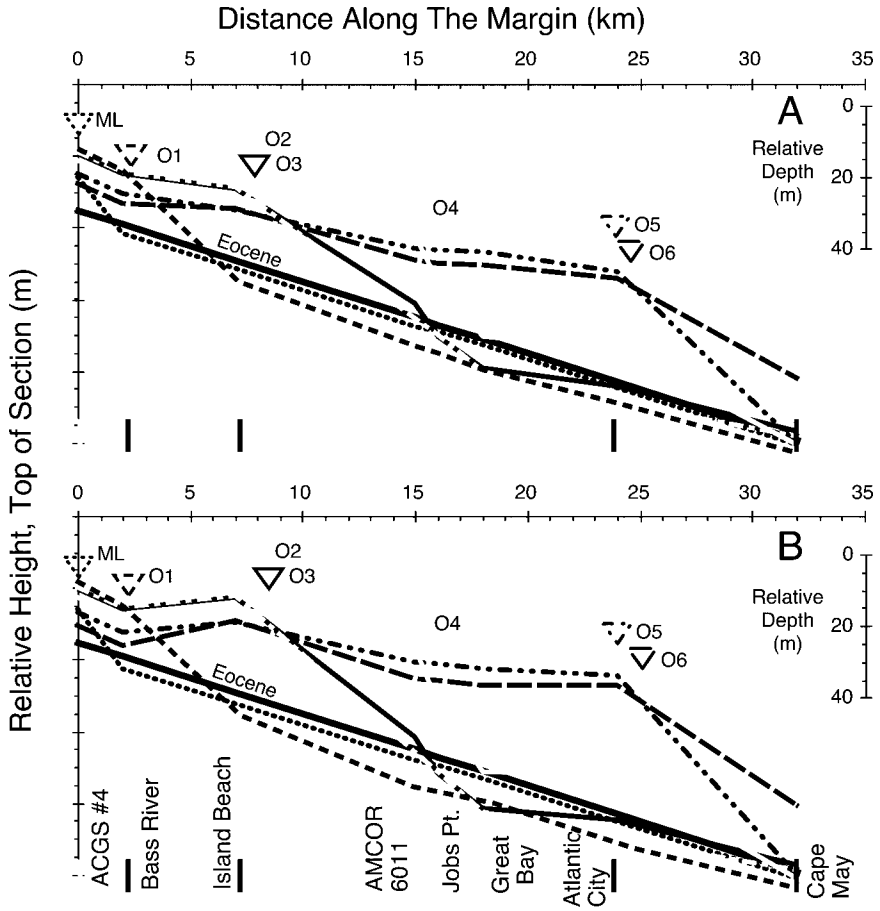

Figure 4. Depth to the sequence boundaries of each of seven Oligocene sequences derived from two-dimensional backstripping. The absolute depth to the top of the Eocene surface (thick black straight line) was not determined, so only relative depths are plotted. The surface geometries generated assuming high porosity vs. depth curves (A) show slightly less variation across the margin as compared to those reconstructed assuming low porosity vs. depth curves (B). Inverted triangles are labeled and keyed to the line patterns. The clinoform break point must occur between this location (maximum sediment thickness) and the adjacent, seaward, borehole.

curves for sandstone and shale (Fig. 3) were taken from estimates at the COST B-2 well (located in Fig. 1; Rhodehamel, 1977; Smith et al., 1976). Porosity estimates for silt and carbonates (rare in the Oligocene, but more important in Mesozoic strata) were from the generic curves of Bond and Kominz (1984). We characterized compaction for each lithology by definition of two exponentially decreasing curves for each following Bond and Kominz (1984; e.g., Fig. 3). The range of porosity observed for each lithology was taken into account by performing the entire analysis, from backstripping through eustatic sea-level estimates, using first a high end-member and then a low end-member set of porosity curves.

We assumed a post-Eocene surface with a gradient of 1:500 based on backstripping of this margin by Steckler et al. (1999). They suggested that this relatively steep gradient was a result of low clastic input prior to latest Eocene time, coupled with tilting due to sediment loading seaward of the hinge line.

The post-Eocene surface subsided through the Oligocene in response to a number of factors. One-dimensional (Airy isostatic) backstripping was used to estimate the compaction of the pre-Oligocene sediments and to estimate the Oligocene sediment thickness and density. These data were used to determine the change in total sediment thickness and the load for flexural calculations.

A two-dimensional flexural model was used to calculate the response of the basement to the Oligocene sediment load. The Oligocene sediment (from both the onshore and offshore wells) was progressively loaded onto an elastic plate. The rigidity was that of a 30-km-thick elastic plate landward of the hinge zone (located at 32 km on our composite cross section). From the hinge zone the rigidity decreased smoothly, in 2.5 km increments, to a 20 km elastic plate thickness near the shelf-slope break (located at 150 km on the composite dip section, Fig. 1). These rigidities were simplified from Steckler et al. (1999). Because the Oligocene was more than 100 m.y. after active extension, this rigidity profile was not varied during this short geologic interval (ca. 34−23 Ma).

In a passive margin setting, tectonic subsidence of the basement generally increases with distance away from the continent. The subsidence beneath the coastal plain, which is landward of the hinge zone, is generated by flexural response to sediment loading of the cooling, stretched, seaward portion of the margin (e.g., Steckler et al., 1988). As such, this component of subsidence was taken into account by the two-dimensional loading model, which included offshore sediment loading. Thus, tectonic subsidence was not included as a separate source of subsidence in this study. Evidence of tectonics unrelated to Mesozoic extension and initiation of the Atlantic Ocean is minor in this region (e.g., Grow et al., 1988). However, it merits serious consideration as we discuss the results of this study, which assumes a purely thermal tectonic regime.

RESULTS

Clinoform Geometry

Two-dimensional backstripping was used to estimate the depth to the top of all Oligocene sedimentary surfaces. The geometry of each surface from updip to downdip and its vertical relation relative to older and younger horizons were calculated. A subset of these, the Oligocene sequence boundaries, is plotted (Fig. 4), and all horizons used in subsequent analyses are tabulated (Table DR2). Clinoform geometries were calculated assuming either maximum or minimum porosity-depth curves (e.g., Fig. 4; Tables DR2 and DR3). The overall progradational nature of the margin is indicated by the progressive migration of the apparent clinoform breakpoint (inverted triangles, Fig. 4) seaward. The clinoform breakpoint must have fallen between the borehole with the thickest succession of each Oligocene sequence and the next borehole seaward. This is indicated by the offset of progressively younger inferred break points at the Island Beach (O2 and O3) and the Atlantic City (O5 and O6) boreholes. Presumably, wedges of sediment corresponding to both se-

quences O2 and O3 occur between the AMCOR 6011 and the Island Beach boreholes. The location of the clinoform break point is only well determined for sequence O4 due to the tight proximity of the AMCOR 6011, Jobs Point, and Great Bay boreholes. We have not extrapolated our data to fit this paradigm, but rather, performed the analyses with only the observed data.

A number of more subtle phenomena were also revealed by the Oligocene stratal geometries (Fig. 4). In many cases, not only did the locus of sedimentation shift seaward with time, but, with the exception of O6, no additional Oligocene sediment accumulated in the western locations after the original depositional episode. As a result, the landward Oligocene sediment surface deepened steadily with time (e.g., the ACGS #4 and Bass River boreholes reach their shallowest depth after deposition of O1 and deepen steadily thereafter). This deepening was strictly a result of the flexural response to sediment loading farther offshore, including deposition of the clinoforms pictured here, and deposition in the region of the offshore wells. Loading due to sedimentation at the offshore wells also required deepening of the Eocene surface seaward of the locus of Oligocene deposition. However, deposition of sediment seaward of the toe of the wedge occurred throughout Oligocene time, maintaining this surface fairly near to the original, pre-Oligocene, depositional surface.

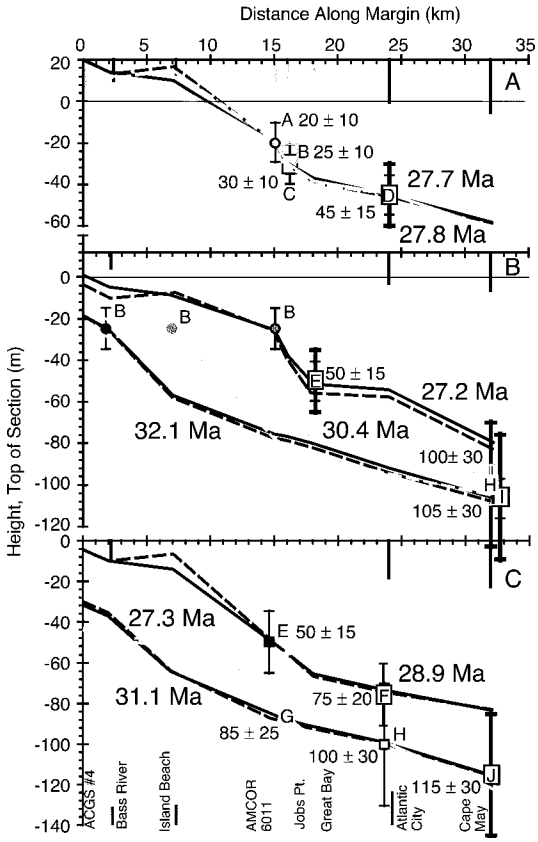

Figure 5. (A) Water-depth ranges of benthic foraminiferal biofacies defined by the sediment surface geometries (Pekar and Kominz, 2001). Solid lines are from high porosity curves (Fig. 3 and Table DR3). Dashed lines are from low porosity curves (Fig. 3 and Table DR3). Benthic biofacies assemblage A (circle) was used to define the depth of each profile. Error bar indicates range of water depth for that benthic biofacies (also printed beside the mid-point in meters). Biofacies depths estimated by correlation along these horizons are given by rectangles and labeled by biofacies (B, C, and D). Narrow error bars on benthic biofacies D are those required by ties to inner neritic biofacies. Thick error bars are required by reduced environmental variation with depth and are used in subsequent modeling. (B) Benthic biofacies assemblage B (circles) was used to constrain the depth of benthic biofacies assemblages E, H, and I. Symbols and line patterns as described in A. (C) Benthic biofacies assemblages F, G, and J were not found in correlative horizons with inner neritic biofacies and were tied to the water-depth ranges of biofacies E and H (small squares). Symbols and line patterns are described in A.

Calibration of Biofacies

While the distribution of benthic foraminifera was constrained by the environmental conditions (e.g., substrate, salinity, temperature, wave energy, oxygenation, and nutrients) in which they lived and not by water depth, environmental conditions are commonly depth dependent (e.g., Bandy, 1953; Walton, 1964). Thus, it is possible to construct a model relating water depth to benthic biofacies (e.g., Nyong and Olsson, 1984; Olsson, 1991; Miller et al., 1997). Because environmental factors become less variable with increasing depth, such a model must become less precise with depth. A new approach to calibration of benthic biofacies to water depth was made possible by the two-dimensional backstripping results. A complete description and analysis of the faunal input, and implications for biofacies of Oligocene age, are beyond the scope of this paper and are presented in Pekar and Kominz (2001). Only a brief synopsis of the results, necessary for calculation of eustatic change, is included here.

Biofacies obtained by factor analyses of Oligocene data provided assemblages dominated by species that generally inhabited inner, middle, or outer neritic environments (Pekar and Kominz, 2001; Table 1).

Three benthic foraminiferal biofacies (A, B, and C) were interpreted as indicating inner neritic environments. Lithostratigraphic relations, previous work on younger, equivalent fauna (Table 1), and low biodiversity (Pekar and Kominz, 2001) all suggest that these biofacies lived in inner neritic environments, and thus in water depths of <30 m. Relative depths were obtained where two different biofacies could be correlated along a single time horizon. Chronostratigraphic correlation was possible due to the tight age control and the sequence stratigraphic framework discussed earlier (Fig. 2). Biofacies A was observed in the Amcor 6011 borehole during early deposition of sequence O4 (Fig. 2). Over the same interval, biofacies B, A, and C were observed in the Jobs Point borehole. By correlating along the backstripped geometry at 27.8 and 27.7 Ma, we found that the surface at the location of Jobs Point was about 10 m deeper than it was at the location of Amcor 6011 during these two times (Fig. 5A). Thus, biofacies B and C were assumed to indicate deeper water depths than biofacies A. The shallowest inner neritic benthic biofacies, A, was assigned a water depth

TABLE 1. BENTHIC FORAMINIFERAL BIOFACIES

Biofacies	Dominant species	References	Depth*	Depth†	Depth§
A	*Cibicides primulus*; *Hanzawaia prona*	Murray (1973); Walton (1964) Schnitker (1970)	Inner neritic	15 0–30	20 10–30
B	*Rectobulimna* spp.; *Cibicides ornatus*	Schnitker (1970)	Inner neritic	15 0–30	25 15–35
C	*Nonionellina* spp.	Walton (1964); Schnitker (1971)	Inner neritic	15 0–30	30 20–40
D	*Bulimina gracilis*	Observed facies associations	Middle neritic	65 30–100	45 30–60
E	*Buliminella elangantissima*	Walton (1964); Schnitker (1970)	Middle neritic	65 30–100	50 35–65
F	*Epistominella pontoni*; *Buliminella curta*; *B. paula*	Walton (1964); Pekar (1999)	Middle neritic	65 30–100	75 55–95
G	*Trifarina bradyi*; *Globocassidulaina california*	Phleger and Parker (1951); Pekar, 1999	Middle neritic to outer neritic	90 30–150	85 60–110
H	*Uvigerina* spp.	Sen Gupta (1971); Kafescioglu (1975)	Outer middle neritic to outer neritic	110 65–155	100 70–130
I	*Globocassidulaina subglobosa*	Observed facies associations	Middle neritic to outer neritic	90 30–150	105 75–135
J	*Trifarina angulosa*; *Globobulimina auriculata*; *G.* spp.	Kafescioglu (1975); Schnitker (1971)	Outer neritic	150 100–200	115 85–145

Note: From Pekar and Kominz (2001).
*Inferred by cited refernces or by observed facies associations and species abundance trends.
†Inferred mean depth and depth range implied by *.
§Mean depth and depth ranges derived in this paper.

of 20 ± 10 m. The deeper inner neritic biofacies were assigned water depths of 25 ± 10 m (B) and 30 ± 10 m (C). These error ranges allowed the water-depth assignments of these benthic biofacies to remain dominantly in the inner neritic zone, and required significant overlap, while allowing minimal differentiation between the three biofacies from the deepest to the shallowest. For all benthic biofacies the range of water-depth uncertainty was designed to generate substantial overlap in the ranges of adjacent benthic biofacies (Table 1 and Fig. 5). The ranges were increased with increasing water depth because variations in environment decrease with depth.

Deeper water biofacies (D−J, Table 1) were assigned water-depth ranges by correlation to inner neritic biofacies based on the sequence stratigraphic model (Fig. 2). The water depth of the inner neritic benthic biofacies (20, 25, or 30 m ± 10 m, see preceding) was used to constrain the depth of the Oligocene surface at the location of the borehole in which it was observed. That is, the geometry of the profile at that time, generated from backstripping (e.g., Fig. 4), was hung from the depth required by the inner neritic biofacies (Fig. 5, A and B). The water depth in which the deeper water biofacies lived could then be estimated. This was possible for biofacies D, E, H, and I (Fig. 5, A and B). For example, benthic biofacies D was preserved in the Atlantic City borehole ca. 27.7 Ma (Fig. 5A). We already used benthic biofacies A preserved at the Amcor 6011 borehole to establish the relative depth of the sediment surface profile at that time, requiring a water depth at the Atlantic City borehole of 45 ± 10 m (Fig. 5A). Because environmental factors change less rapidly with depth, we did not assume that benthic biofacies D lived in the tight range of depths inferred by this correlation. Instead we increased the inferred depth range to 45 ± 15 m (Fig. 5A). The depth of deposition of biofacies E, H, and I were all constrained by correlation along backstripped sediment surface geometries to benthic biofacies B (Fig. 5B). The uncertainty of water depth for biofacies E, like that of D, was increased to ±15 m. Biofacies H and I are outer middle to outer neritic and thus were assigned larger depth ranges of ±30 m.

Biofacies F, G, and J were not sampled at a time of coeval deposition of inner neritic biofacies. However, biofacies F was correlated to biofacies E, while biofacies G and J were tied to biofacies H (Fig. 5C). In most cases, the water-depth ranges assigned to biofacies were considerably larger than the uncertainty in water depth required by the calibration (Fig. 5).

The impact of using high versus low porosity assumptions was generally small (Fig. 5). In cases where the results differed (a maximum of 10 m for the calibration of biofacies H at 30.4 Ma), the average of the two was used to estimate the water depth associated with that benthic biofacies assemblage. An uncertainty of 5 m in the best estimate of the paleowater depth for biofacies H is modest compared to the range in uncertainty of ±30 m assigned to this outer middle neritic biofacies. Our resulting depth estimates for the 10 benthic biofacies (Table 1) relate favorably to changes in species diversity, to faunal abundance, and to previous studies (Pekar and Kominz, 2001).

Sea-Level Calculations

Two-dimensional backstripping established the geometry of the Oligocene surfaces (Table DR2), while the water-depth ranges of benthic foraminiferal biofacies (Table 1) were used to determine if base-level changes occurred. In the absence of modeling errors, any variation in water depth established by the biofacies and inconsistent with the two-dimensional backstripping results required a relative sea-level change. The observed inconsistencies are referred to as R2, the second reduction of Bond et al. (1989). Water loading due to eustasy increases the water depth by a factor of about 1.48 (the density of mantle, 3.18 g/cm^3, divided by the density of the mantle less the density of seawater). Thus, sea-level change is equivalent to R2/1.48. In the case of a profile generated by two-dimensional backstripping, if two or more benthic biofacies at different locations along that profile require consistent sea-level change, then this suggests that local tectonics were not active and that the observed R2 change was due to eustasy. Our approach to estimating R2 and sea-level change is illustrated by a detailed consideration of sequence O2 (Fig. 6).

Detail of Method: Sequence O2

The clinoform wedge of sequence O2 was sampled at the Island Beach borehole. Offshore time-equivalent, deep-water strata were sampled at both the Atlantic City and Cape May boreholes. Four benthic biofacies picks at Island Beach, two at Atlantic City, and three at Cape May (Fig. 2A) were used, in conjunction with backstripped geometries (Tables DR2 and DR3), to define R2 changes.

The transgressive systems tract of sequence O2 was sampled in both the Cape May and the Atlantic City boreholes. The Cape May basal sediments contain biofacies J (115 ± 30 m), whereas those at Atlantic City contain biofacies H (100 ± 30 m; Fig. 6A; Table DR4). Wherever correlative well data are constrained by benthic biofacies, the shallower estimate was used as our preliminary constraint on R2, because the shallower biofacies generally had narrower depth ranges. The backstripped profile at 31.7 Ma (the base of the sequence) was hung on biofacies H at Atlantic City. The change to the maximum flooding surface profile (from ca. 31.7 to 31.1 Ma) required by backstripping (dashed white line; Fig. 6A) was compared to the same profile hung on

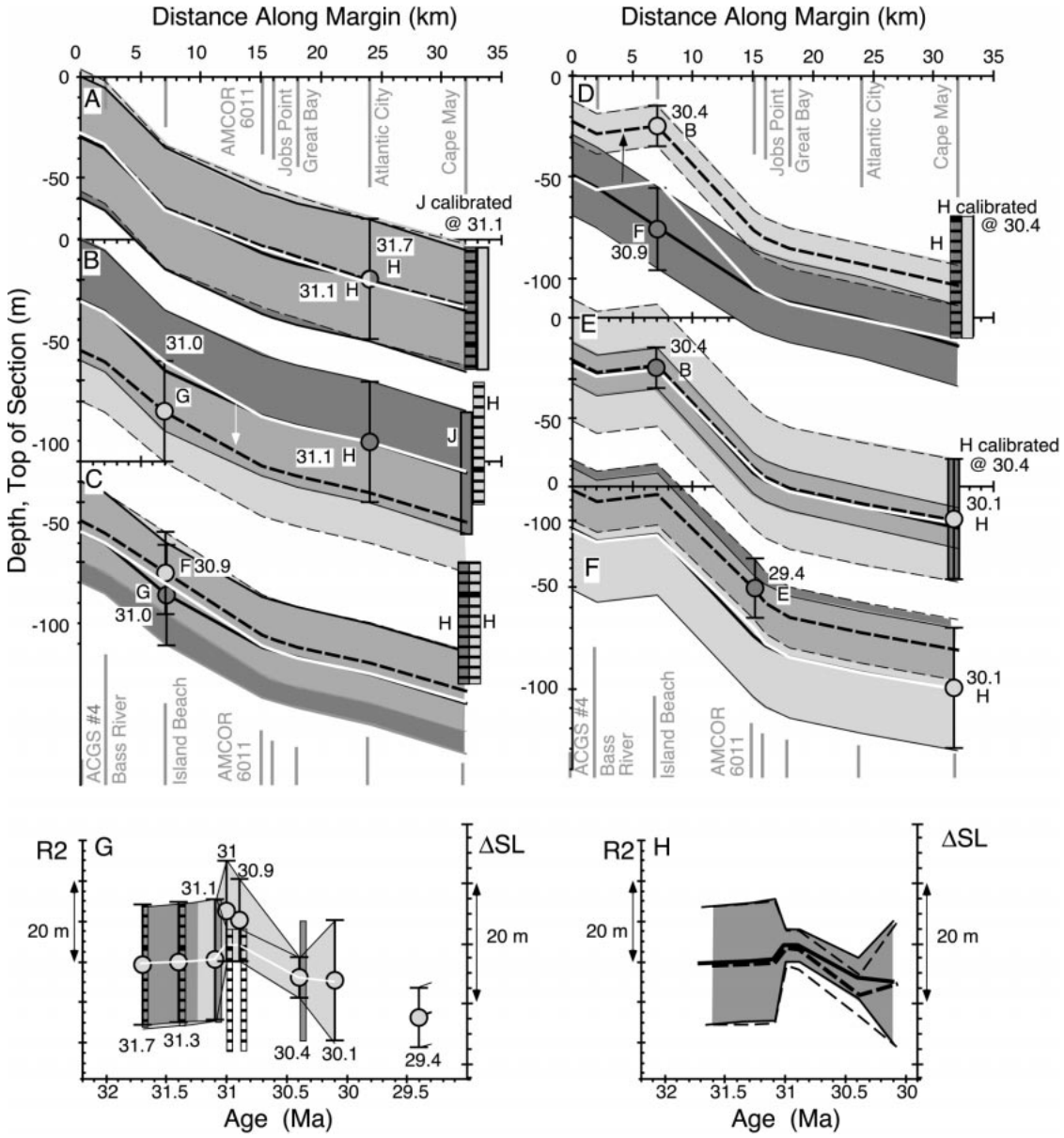

Figure 6. Detailed example of the generation of R2 and eustatic estimates from two-dimensional backstripping, sequence O2. (A−F) The geometry of two consecutive time horizons. Circles with error bars show the water depth ranges of the benthic biofacies (indicated by a letter, e.g., G and H) used to hang the cross section. The range of water depths of the older horizon is indicated by solid black lines. The depth range is shaded dark gray. The depth range of the younger horizon is indicated by dashed black lines shaded light gray. The overlap of the two ranges is medium gray (a lack of change results in almost exclusively medium gray in A). White dashed lines give the depth of the younger horizon relative to the older horizon, as determined by backstripping alone. The difference between the white dashed line and the bold (mid-point) black dashed line is R2 (white arrow in B, essentially zero in A). Where benthic biofacies were observed in two locations at a single time, correlative benthic biofacies are indicated by a vertical rectangle. The height of the rectangle represents the depth range of that benthic biofacies and the horizontal location is the well in which it was identified. Bars filled by gray indicate that the water depth range of that benthic biofacies was established by this correlation (e.g., J in B). Horizontally striped bars indicate that this correlation can be used to corroborate and/or to constrain water depths required by the benthic biofacies used to hang the section (e.g., H in B). Rectangular bars are dark gray if these biofacies correlate with the older horizon and light gray if they correlate with the younger section. Approximate ages (Ma) are shown. The resulting R2 changes (left scale) are summarized in G. The ΔSL, or eustasy (right scale), is calculated from R2 by removing the effects of water loading. Present-day sea level was not tied to eustasy. Correlative biofacies ca. 31.1 and 30.4 Ma were used to establish the water depth ranges of biofacies J and H, respectively (see Fig. 5). No correlative biofacies were present ca. 30.1 and 29.4 Ma. Correlative biofacies ca. 31.7 and 31.3 Ma corroborated water depths. Correlative biofacies ca. 31.0 and 30.9 Ma placed considerable constraint on R2 estimates. The constrained, best-estimate R2 and sea-level curves are indicated by the white line with dark gray shading of uncertainty ranges. These results were obtained using the high porosity curves. Dashed lines in H show the constrained R2 and eustatic results assuming low porosity vs. depth curves.

biofacies H at Atlantic City (dashed black line, Fig. 6A). There was essentially no difference in the two 31.1 Ma profile depths. Thus, no change in R2 was required between ca. 31.7 and 31.1 Ma.

Immediately above the maximum flooding surface there was an abrupt facies deepening at the location of the Island Beach borehole. Although we had no biofacies data below the maximum flooding surface in the Island Beach borehole, constraints from fauna at the Atlantic City borehole required a water depth of between 35 and 85 m (dark and medium gray, Fig. 6B). The backstripping geometry requires a very slight shoaling at the Island Beach borehole between ca. 31.1 and 31.0 Ma (white dashed line compared to the thick black line, Fig. 6B). However, benthic biofacies G occurs here, suggesting a distinct deepening (R2 change of −30 m to +80 m deeper) between ca. 31.1 and 31.0 Ma (light and dark gray, Fig. 6G).

Benthic biofacies F was sampled above the maximum flooding surface at the Island Beach borehole. A slight shoaling was required by the backstripped data at this borehole (Fig. 6C). The shoaling indicated by the fauna was slightly less than that suggested by backstripping, suggesting a reduction in water depth (R2 fall, Fig. 6C).

The highstand portion of sequence O2 sampled at Island Beach continued to shoal into biofacies assemblage B (25 ± 10 m, Fig. 6D). By the end of deposition at the Island Beach borehole, ca. 30.4 Ma, significant shoaling was required (gray dashed line, Fig. 6D). The change in benthic biofacies and increase in sedimentation together required an R2 fall of about 28 m. This change is assumed to be present for the entire profile, although it is only required by the benthic biofacies in the Island Beach well. The youngest O2 strata were sampled only in toe of slope deposits at the Cape May borehole. The associated biofacies, H (100 ± 30 m) was used to constrain the surface profile at that time. There was essentially no change in R2 required between ca. 30.4 and ca. 30.1 Ma O2 (Fig. 6E).

Determination of R2 changes across sequence boundaries is simpler than within sequences because there is no change in the sequence boundary geometry and, thus, no change required by backstripping. Benthic biofacies E in the AMCOR 6011 borehole, during early deposition of sequence O2b, suggests a possible drop in R2 relative to the same profile at the end of deposition of sequence O2 (Fig. 6F).

Many of the surfaces used to constrain R2 changes in sequence O2 contained correlative biofacies assemblages (Figs. 2A and 6). In two cases, these correlations were used to establish the water-depth ranges of specific faunal assemblages. The water depth of biofacies J was established at the maximum flooding surface, ca. 31.1 Ma (light gray column at the Cape May borehole, Fig. 6A). The water depth of biofacies H was established at 30.4 Ma (Fig. 6D). Overlapping ranges were used to restrict the possible range of R2 changes in all other cases in which two or more biofacies correlated.

Benthic biofacies were sampled at two boreholes just above the maximum flooding surface (ca. 31.0 Ma, Fig. 6B). Benthic biofacies G at Island Beach (60–110 m) requires a water-depth range at Cape May of 114−164 m, while the presence of biofacies H at Cape May indicates a depth range of 70−130 m. The two constraints together suggest a probable water-depth range of 114−130 m at Cape May, and 60−76 m at Island Beach. A similar correlation of benthic biofacies F at Island Beach with H at Cape May ca. 30.9 Ma restricts the range of water depths in those locations to 75−92 m and 113−130 m, respectively (Fig. 6C). Benthic biofacies J at the Cape May borehole correlated with benthic biofacies H at the Atlantic City borehole at the base of sequence O2 (Fig. 6A). These two biofacies were entirely consistent and resulted in no reduction in the uncertainty of the depth ranges.

The resulting R2 values estimated for sequence O2 are were plotted at the same scale in Figure 6G (Table DR4). The water-depth changes could not be tied to present sea level. The resulting eustatic curve was obtained by removing the water loading (Table DR4).

The entire analysis described here was obtained assuming maximum compaction (high porosity curves, Fig. 3, and Bond and Kominz, 1984). When minimum porosity versus depth curves were used to determine R2, the results were nearly identical (Fig. 6H, dashed lines). Why were the results the same? First, R2 changes were largely constrained by the biofacies, not by compaction calculations. However, the biofacies depth ranges were constrained by the backstripping results. The biggest variation, about 3 m ca. 30.4 Ma, occurred where benthic environmental controls were inner neritic biofacies B on a very thick sediment wedge at Island Beach. That variation in model results using high versus low porosity curves accounts for the fact that to calibrate H (ca. 30.4 Ma), an average depth was required from application of the two different compaction schemes (Fig. 5B).

R2 Calculations and Results

The constraints on sea level resulting from this analysis are summarized in Table DR4 and Figure 7. Table DR4 includes details of the analyses and constraints on R2 assuming high porosity curves. Only the final results are given for both low and high porosity assumptions because the constraints were identical and the results were nearly identical (Table 2 and Fig. 7B).

Eocene (34 Ma)

Two-dimensional paleoslope modeling of the uppermost Eocene (Browning et al., 1997; Pekar et al., 2000) in an updip well (Medford) suggested an outer neritic environment for the uppermost Eocene sequence at the ACGS #4 borehole (Pekar and Kominz, 2001). Thus, we assigned a water depth of 100 ± 30 m to the top of the Eocene.

Sequence ML (Mays Landing)

The ML sequence was only observed at the ACGS #4 borehole. Benthic foraminiferal biofacies were not analyzed due to poor preservation of microfossils. Inner neritic water depths (20 ± 20 m) were indicated by the lithostratigraphy at the base of the ML sequence, requiring a significant decrease in water depth (R2 change) of 75 m relative to the Eocene surface (Fig. 7; Table DR4). An abrupt deepening to middle neritic water depths (60 ± 20 m) indicated by the lithostratigraphy (Pekar, 1999) was followed by a gradual shoaling to inner neritic environments at the top of the ML sequence. The required R2 rise of ~40 m and subsequent fall of ~25 m were assigned large uncertainties due to the lack of biofacies control in this well. Clearly, results from this sequence are poorly defined.

Sequence O1

The R2 signal of sequence O1 was defined by 11 biofacies estimates from the Bass River borehole, 1 from the Island Beach borehole, and 2 from the Cape May borehole. Outer neritic facies H at Island Beach was interpreted as being near the maximum flooding surface. This required a rapid water-depth rise relative to the basal sequence established by inner neritic facies B at Bass River (Fig. 7 and Table DR4). For most of the remainder of sequence O1 water-depth changes (R2) were obtained from the biofacies analyses from the Bass River borehole. These biofacies indicated a number of shifts in environment from inner to middle neritic (Fig. 2A). A higher frequency, orbital control on eustatic change is possible (e.g., Pekar, 1999). Our analyses suggested generally deeper water depths in the lower portion of sequence O1 followed by an abrupt shallowing ca. 32.3 Ma (Fig. 7). The inner neritic biofacies B at Bass River used to constrain this eustatic fall was consistent with

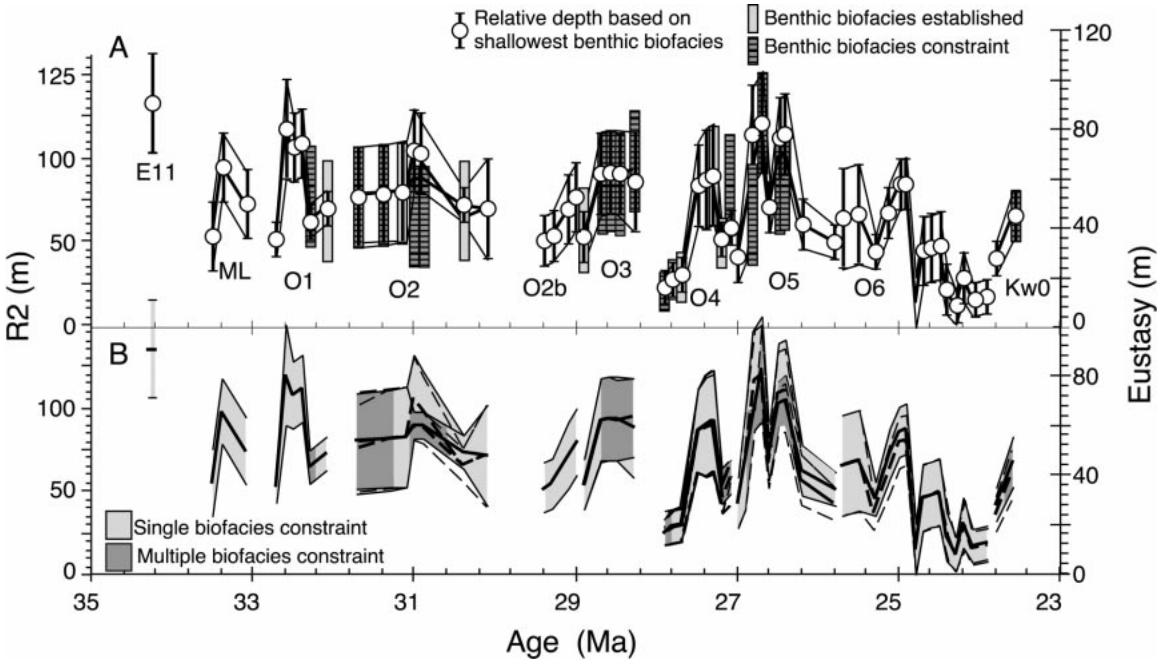

Figure 7. (A) R2 results, and the data on which they were based. The vertical bars indicate multiple biostratigraphic constraints along a single horizon. Benthic biofacies depth ranges were defined (light gray, vertical bars) in 7 cases, and in 16 cases, multiple benthic biofacies reduced or confirmed the ranges of R2 (dark gray, striped, vertical bars). The thick black line is the mean R2 result, without constrained error bars. These results were obtained using high porosity curves for all lithologies. Eustasy (right side vertical scale) is estimated by removing the water load. Values are relative to the minimum value in this data set. They are not tied to present-day sea level. (B) R2 results. Light gray shading of ranges represents the R2 values required by only the shallower benthic biofacies. Dark gray shading gives the reduced range of R2 assuming high porosity-depth relations (A). Dashed black lines superimposed on the shaded results are the R2 results calculated using low porosity curves for all lithologies.

correlative outer neritic biofacies at Cape May, confirming the biofacies model but placing no constraints on eustasy. The Cape May borehole also contains youngest O1 sediments. The depth range of biofacies I was established here by correlation to inner neritic biofacies B observed in the Bass River borehole (Fig. 5 and Table DR4).

Sequences O2 and O2b

The calculation of R2 and eustasy from the sequence O2 data were discussed in detail above. Eustatic changes required by these data were moderate. There was an indication of a sea-level fall in the latter half of the sequence, but a sea-level rise was not required by the model results (Figs. 6G and 7). An additional sequence, O2b, was recognized by Pekar et al. (2000) and was partially sampled by the AMCOR 6011 and Jobs Point boreholes. Two O2b biofacies estimates were available in each of these boreholes, although data from the Jobs Point borehole were poor (Pekar and Kominz, 2001). These data suggested a shoaling since the end of deposition of sequence O2 followed by a moderate rise during deposition of the O2b strata.

Sequence O3

Although the clinoform portion of sequence O3 was not observed in this data set, it was well represented by middle to outer neritic facies in the AMCOR 6011, Atlantic City, and Cape May boreholes. All horizons used in sequence O3 contain correlative biofacies from multiple boreholes. Biofacies F was assigned its depth range at the base of the section (ca. 28.9 Ma). The remainder of the correlations confirmed the water depths of correlative benthic biofacies, constraining those depths by small amounts (Fig. 7 and Table DR4). An eustatic fall was suggested between sequence O2b and sequence O3, followed by a moderate rise and then nearly constant sea level through the remainder of this sequence.

Sequence O4

Sequence O4 samples included portions of both the thick clinoform wedge and the toe of slope deposits. The clinoform wedge of sequence O4 was sampled at the AMCOR 6011 well and constrained by five inner neritic benthic biofacies (Fig. 2A). The Jobs Point well contained a thick O4 sequence with mixed inner and middle neritic biofacies (Fig. 2A). Middle neritic biofacies were sampled at the top of the O4 sequence in the Great Bay borehole, and the Atlantic City borehole recovered dominantly middle to outer neritic biofacies (Fig. 2A). In most cases, horizons were constrained by inner neritic facies of the AMCOR well. These were used to calibrate the water-depth ranges of biofacies C, D, E, and G (Fig. 5 and Table DR4). Correlation ca. 27.1 of biofacies B at AMCOR 6011 with biofacies G at Atlantic City reduced the uncertainty in R2 by nearly half (Table DR4 and Fig. 7A). Biofacies E, present at the same time in the Great Bay borehole, was consistent with this reduction. The resulting sea-level event showed a fairly steady, low, sea level (some 40 m below the end of O3 deposition) with a rapid rise (about 40 m) to the maximum flooding surface ca. 27.4 Ma. A subsequent fall of about 30 m may have been followed by another minor rise at the end of sequence O4.

Sequence O5

The clinoform wedge of sequence O5 was sampled at the Jobs Point, Great Bay, and Atlantic City boreholes. Some correlative toe of slope deposits were also cored at Cape May.

Four horizons included correlative biofacies. The correlation of those biofacies placed considerable constraint on the R2 curves (Fig. 7 and Table DR4). The overall result suggested two rapid rises and falls of sea level. The sequence began with a rapid sea-level rise of nearly 50 m followed by an abrupt 35 m fall and a rapid 23 m rise. Subsequent minimal change for a short period was followed by an abrupt 30 m fall and slow continued shoaling of ~5 m to the end of this sequence.

Sequence O6

There were no time horizons with correlative biofacies data in sequence O6. Minor occurrences of this sequence obtained in the Island Beach and Atlantic City boreholes were interpreted as the remains of transgressive systems tracts. This sequence was well sampled by the Cape May Borehole, and 18 benthic biofacies samples indicate the presence of higher frequency variations in water depth (parasequences; Pekar, 1999). These parasequences were used in conjunction with Sr isotope stratigraphy to estimate ages in this sequence (Pekar, 1999). They were also readily identified in the R2 model results with an implied maximum eustatic fall as great as 47 m ca. 24.9 Ma, and as small as 10 m ca. 24.2 Ma.

Lowermost Miocene Kirkwood (Kw0)

We included an analysis of the lowest part of the Kirkwood Formation in order to tie our results with the Miocene record. Kw0 was sampled at the Atlantic City and Cape May boreholes (Pekar, 1999; Pekar and Kominz, 2001). No tightening of uncertainties in R2 results was required by correlative biofacies ca. 23.6 Ma. Our analysis suggested that the Miocene sea level was somewhat higher than that at the end of the Oligocene and continued to rise during the deposition of this portion of this sequence.

TABLE 2. EUSTASY

Seq.	Approx. age (Ma)	High porosity vs. depth			Low porosity vs. depth			Eustasy*		
		Minimum	Mean	Maximum	Minimum	Mean	Maximum	Minimum	Mean (m)	Maximum (m)
E11	34.2	70.7	91.0	111.3	70.9	91.2	111.4	70.7	91.1	111.4
ML	33.5	23.4	36.9	50.4	23.6	37.1	50.6	23.4	37.0	50.6
ML	33.4	52.3	65.8	79.4	52.5	66.1	79.6	52.3	66.0	79.6
ML	33.1	36.3	49.8	63.3	36.4	49.9	63.4	36.3	49.9	63.4
O1	32.9	29.0	35.7	42.5	28.7	35.5	42.2	28.7	35.6	42.5
O1	32.7	29.3	36.1	42.8	29.1	35.9	42.6	29.1	36.0	42.8
O1	32.6	60.2	80.5	100.7	60.2	80.5	100.8	60.2	80.5	100.8
O1	32.5	59.0	72.5	86.0	58.8	72.3	85.8	58.8	72.4	86.0
O1	32.4	61.5	75.0	88.6	61.4	75.0	88.5	61.4	75.0	88.6
O1	32.3	37.0	43.8	50.6	36.9	43.7	50.5	36.9	43.7	50.6
O1	32.1	41.9	48.7	55.5	41.9	48.7	55.4	41.9	48.7	55.5
O2	31.6	35.1	54.7	74.2	34.7	54.1	73.4	34.7	54.5	74.2
O2	31.3	35.3	55.3	75.3	34.9	54.8	74.7	34.9	55.1	75.3
O2	31.1	35.4	55.7	76.0	35.0	55.3	75.6	35.0	55.5	76.0
O2	31.0	54.4	60.3	66.1	55.1	60.5	65.8	54.4	60.3	66.1
O2	30.9	53.4	59.8	66.3	54.7	60.4	66.0	53.4	59.8	66.3
O2	30.4	37.9	44.7	51.4	42.7	49.4	56.2	37.9	47.1	56.2
O2	30.1	27.9	48.2	68.5	27.8	48.1	68.4	27.8	48.2	68.5
O2b	29.4	25.4	35.5	45.7	24.8	34.9	45.1	24.8	35.2	45.7
O2b	29.3	26.7	36.8	46.9	26.2	36.4	46.5	26.2	36.6	46.9
O2b	29.1	34.8	48.3	61.8	33.6	47.2	60.7	33.6	47.7	61.8
O2b	29.0	36.8	50.4	63.9	39.8	53.3	66.8	36.8	51.8	66.8
O3	28.9	26.7	36.8	46.9	26.3	36.4	46.5	26.3	36.6	46.9
O3	28.7	46.5	62.9	79.2	46.1	62.6	79.1	46.1	62.6	79.2
O3	28.6	46.8	63.3	79.7	46.4	63.1	79.7	46.4	63.1	79.7
O3	28.5	46.3	62.4	78.5	46.4	62.4	78.4	46.3	62.4	78.5
O3	28.3	47.6	63.6	79.6	47.4	63.5	79.6	47.4	63.5	79.6
O4	27.9	12.2	17.6	22.9	12.2	17.2	22.2	12.2	17.6	22.9
O4	27.8	12.8	19.5	26.3	12.9	19.7	26.4	12.8	19.6	26.4
O4	27.7	13.3	20.1	26.8	13.7	20.5	27.2	13.3	20.3	27.2
O4	27.5	41.6	58.5	75.4	41.4	58.3	75.2	41.4	58.4	75.4
O4	27.4	39.6	59.9	80.2	40.0	60.3	80.6	39.6	60.1	80.6
O4	27.3	41.2	61.4	81.7	41.9	62.2	82.5	41.2	61.8	82.5
O4	27.2	25.2	32.0	38.7	28.3	35.1	41.9	25.2	33.5	41.9
O4	27.1	37.4	39.8	42.2	38.9	42.6	46.2	37.4	41.8	46.2
O5	27.0	19.6	29.8	39.9	18.9	29.1	39.2	18.9	29.4	39.9
O5	26.9	26.3	46.6	66.8	26.1	46.4	66.7	26.1	46.5	66.8
O5	26.8	58.4	62.6	66.8	57.9	62.3	66.7	57.9	62.4	66.8
O5	26.7	62.3	81.8	101.2	63.5	83.4	103.3	62.3	82.8	103.3
O5	26.6	35.0	45.1	55.2	38.2	48.3	58.5	35.0	46.7	58.5
O5	26.5	56.5	65.9	75.4	60.1	68.9	77.8	56.5	67.1	77.8
O5	26.4	57.6	67.6	77.6	61.0	70.8	80.6	57.6	69.1	80.6
O5	26.2	28.4	38.5	48.7	31.8	42.0	52.1	28.4	40.2	52.1
O5	25.8	22.4	29.2	36.0	28.0	34.7	41.5	22.4	32.0	41.5
O6	25.7	24.4	44.6	64.9	24.0	44.3	64.5	24.0	44.5	64.9
O6	25.5	25.9	46.2	66.5	25.8	46.1	66.4	25.8	46.1	66.5
O6	25.3	18.4	25.2	32.0	23.9	30.6	37.4	18.4	27.9	37.4
O6	25.1	33.0	43.1	53.3	38.6	48.8	58.9	33.0	45.9	58.9
O6	25.0	43.5	53.6	63.8	47.5	57.6	67.7	43.5	55.6	67.7
O6	24.9	44.6	54.7	64.9	48.9	59.0	69.2	44.6	56.9	69.2
O6	24.8	0.0	10.1	20.3	0.0	10.1	20.3	0.0	10.1	20.3
O6	24.7	17.6	31.1	44.7	17.6	31.1	44.6	17.6	31.1	44.7
O6	24.6	18.8	32.3	45.8	18.7	32.2	45.7	18.7	32.3	45.8
O6	24.5	20.0	33.5	47.0	19.7	33.3	46.8	19.7	33.4	47.0
O6	24.4	5.5	15.7	25.8	5.1	15.3	25.4	5.1	15.5	25.8
O6	24.3	1.1	7.9	14.7	1.2	7.9	14.7	1.1	7.9	14.7
O6	24.2	10.2	20.3	30.5	10.8	20.9	31.1	10.2	20.6	31.1
O6	24.1	4.0	10.7	17.5	4.7	11.4	18.2	4.0	11.1	18.2
O6	23.9	5.2	12.0	18.8	6.2	13.0	19.7	5.2	12.5	19.7
KwO	23.8	17.2	23.9	30.7	22.0	28.8	35.6	17.2	26.4	35.6
KwO	23.6	30.6	40.8	50.9	35.5	45.7	55.8	30.6	43.2	55.8

Note: These valuse are not tied to present sea level.
*Final eustatic values used are the maximum range of those generated with high or low porosity curves.

DISCUSSION

Estimation of eustasy using this two-dimensional backstripping approach has a number of clear advantages. The main advantage is the potential to test for internal consistency. Internal consistency was tested whenever two or more independently calibrated benthic biofacies correlated along a single horizon. This occurred on 16 horizons in our analysis (Figs. 7 and 8). In our model, the Eocene coastal plain surface gradient was assumed to be 1:500. By assuming steeper (1:300) or flatter (1:1000) gradients, correlative benthic biofacies were not internally consistent (Pekar, 1999). That is, correlative benthic biofacies required water depths outside of the range of the shallower benthic biofacies. The internal consistency of our results also indicates that no high-frequency, short-wavelength tectonics occurred in this region. The presence of active faulting would be expected to result in irreconcilable variations between wells (e.g., Heller et al., 1982). If the sea-level changes that we report are a result of the response of the rigid lithosphere to variations in in-plane stress, then there is an additional slope predicted along our cross section. For example, apparent sea-level rises would be associated with extension, and water

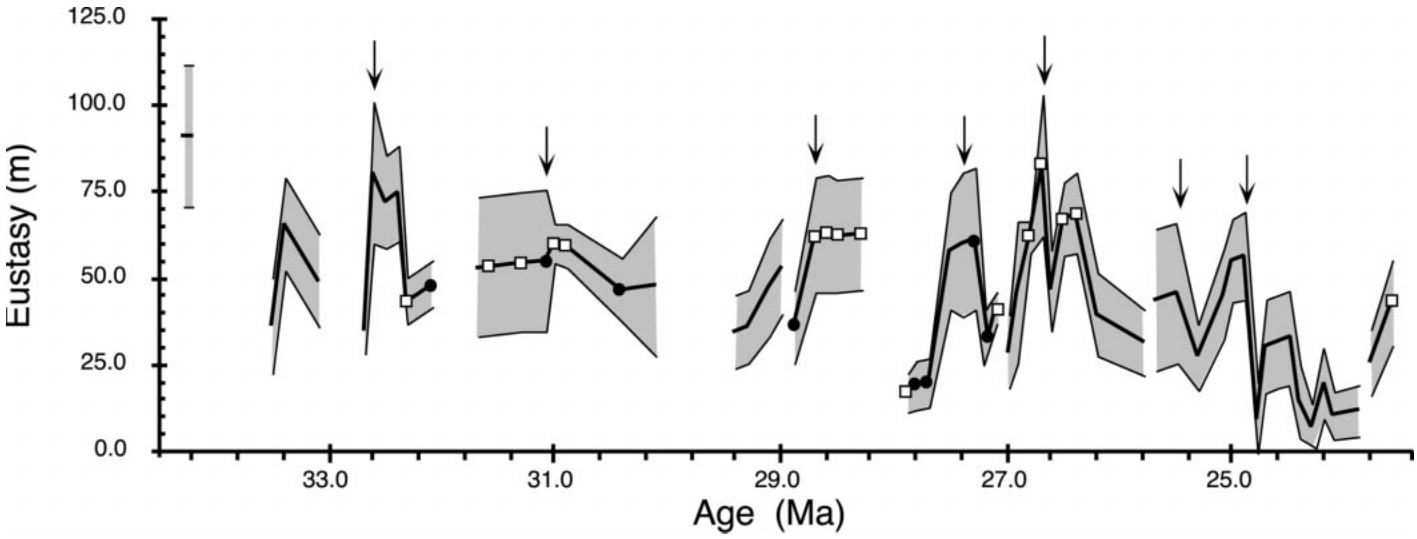

Figure 8. Eustatic curve for the late Paleogene (34−23 Ma). Magnitudes of sea-level change were reduced by multiple correlative benthic biofacies (e.g., dark gray of Fig. 7). However, the maximum ranges of constrained sea level calculated from both high and low porosity curves were used (Fig. 7B; Table 2). Open squares show eustatic values confirmed by two or more independent, benthic biofacies. Filled circles indicate times where depth ranges of benthic biofacies were established. Arrows indicate the positions of the maximum flooding surfaces from the sequence stratigraphic framework used to generate these results (Fig. 2). The variations in eustasy are not tied to present-day sea level.

depths should have been deeper at Cape May than at Bass River (e.g., Cloetingh, 1986). A detailed look at these relations (Table DR4) shows no relationship between the sign of the eustatic change and the relative depths of correlative biofacies. Furthermore, there is no relationship between the magnitude of sea-level change and the magnitude of the water-depth differences inferred along a given horizon. Thus, the two-dimensional approach seems to rule out the possibility that the eustatic variations have any relationship to in-plane stress. Our analyses cannot rule out large-scale tectonics (e.g., Lithgow-Bertelloni and Gurnis, 1997). However, there is no indication of such tectonics in this region (e.g., Grow et al., 1988). We submit that within the uncertainty in compaction, in age dating, and in the depth ranges of benthic biofacies, we have captured the magnitude and timing of third-order eustatic variations, which occurred from latest Eocene to earliest Miocene time (Fig. 8). These magnitudes are not tied to present sea level.

The long-term trend in eustasy within the late Paleogene was an overall fall of ~75 m from latest Eocene to the latest observed Oligocene strata. During this time interval ~8.5−20 m of sea-level fall was possible from decreasing ocean ridge volume (Kominz, 1984). The initiation of the collision of India with Asia began ca. 50 Ma and may contribute a small amount to the observed eustatic fall (e.g., Harrison, 1990). Cooling of the Cretaceous Pacific volcanism also requires a sea-level fall over this time interval (Schlanger et al., 1981). At the same time there is some suggestion of a significant cooling of ocean water, which may have generated a sea-level fall of 2−5 m (Sahagian, 1988). Thus, of this overall 75 m fall, 12.5−29 m can be accounted for by known ocean-volume changes. This suggests that 62−46 m of sea-level drop must be accounted for by changes in glacial ice or other undetermined mechanisms. Full glaciation of East Antarctica would be required during a significant portion of the Oligocene if ice alone generated this fall. This interpretation is consistent with evidence from both benthic and planktonic foraminiferal $\delta^{18}O$ records (Miller and Fairbanks, 1985b; Miller et al., 1991; Pekar and Miller, 1996; Pekar, 1999) and with evidence of significant glaciation in Antarctica at this time (Zachos et al., 1992a, 1992b).

The individual Oligocene sequences each suggest a rise and fall of eustasy. Two exceptions to this, sequence O2b and O3, were poorly sampled by this data set. Higher frequency variations are suggested in sequences O6, O5, and O1. These high-frequency variations are not required in sequence O1 due to uncertainties in water depths of benthic biofacies. In general, third-order variations in sea level are 10−40 m, which can be accounted for by variations in Antarctic ice volume. It is important to note that we have not sampled the complete sequence; the correlative, deep-marine portion of each sequence is missing. It is likely that eustasy fell further during hiatuses. The largest sea-level changes within the observed Oligocene sequences may require nearly complete Antarctic glaciation (e.g., note eustatic changes ca. 33.5, 32.8–32.9, 27.7–27.9, 24.8, and 23.9 Ma, Fig. 8).

It is interesting to note that the highest eustatic values in most sequences are associated with maximum flooding surfaces (arrows in Fig. 8). Sequence stratigraphic paradigms suggest that the maximum flooding surface is associated with the maximum rate of sea-level rise (Posamentier and Vail, 1988). We postulate that in a region like this in which rates of tectonic subsidence (due to offshore loading here) are low, it is eustatic change and not the rate of eustatic change that has the greatest impact on the generation of the maximum flooding surface.

The relationship between the ages of the Oligocene sequences and those defined by global correlation by Haq et al. (1987) was discussed by Pekar et al. (2000) and Miller et al. (1996, 1998b), among others. As was the case for one-dimensional estimates of sea-level change (Kominz et al., 1998), we find that the magnitudes of eustatic change required by our model are considerably less than those suggested by Haq et al. (1987). This is particularly the case for the early Oligocene portion

of the record and for Haq et al.'s (1987) 30 Ma, ~100 m eustatic fall. This fall occurs during the largest hiatus in our data set (between sequences O2 and O2b). However, there is no indication in our data of a significant eustatic fall. The eustatic magnitudes reported by Haq et al. (1987) for the late Oligocene (~50–60 m) are consistent with the highest magnitudes of eustatic sea-level change obtained in this study.

The magnitudes of eustasy suggested by Pinous et al. (1999) based on stratigraphic data from the Aral Sea and north Usturt trough are consistent with our results. Although Pinous et al. (1999) did not assign actual magnitudes to their eustatic changes, the major fall that they showed is during the change from Eocene to Oligocene time. They observed fewer Oligocene sequences than were observed in the New Jersey coastal plain.

The advantages of the two-dimensional backstripping approach are readily apparent when one considers the one-dimensional results of Kominz et al. (1998). Where sequences are present in each well, the one-dimensional approach allows an estimate of eustatic change within the range of uncertainty of benthic biofacies. Benthic biofacies interpretations are not constrained by one-dimensional backstripping, and thus have larger ranges of uncertainty than possible with the two-dimensional approach. Even where correlative strata are available, it is impossible to use the shallower benthic biofacies to constrain the uncertainty in water depths. The two-dimensional approach allows integration of all of the data into a single, internally consistent, interpretation of sea-level change. Limitations of the model include the need for a detailed, two-dimensional database, including lithologies, compaction estimates, flexural rigidity, age, and water depth, integrated into a sequence stratigraphic framework. In addition, when the data set is limited in space (as in the current case), large-scale (e.g., mantle) tectonics could play a role in generating the observed variations.

CONCLUSIONS

A new method for estimating eustasy was successfully implemented for the late Paleogene (34–23 Ma). This method applied two-dimensional backstripping to a detailed sequence stratigraphic database from the New Jersey Oligocene coastal plain. Minor uncertainties in calculated eustatic results due to major variations in assumed porosity versus depth curves were incorporated. Internal consistency of benthic foraminiferal biofacies across correlative horizons demonstrated that the results were robust. It also suggested that neither local tectonics nor in-plane stress changes were operative in this setting during this time interval.

A major sea-level fall is required across the Eocene-Oligocene boundary with overall, continued shoaling to the end of the Oligocene. This requires significant Antarctic glaciation during much of Oligocene time. Individual Oligocene sequences, lasting 0.5–1.5 m.y., reveal sea-level rises and falls, generally of 40 m or less. Higher frequency sea-level variations are observed in some sequences, suggesting that more detailed sampling could allow modeling on this scale.

A number of problems to be undertaken in the near future are suggested by this work. The method could be applied to a more detailed data set. In particular, additional data from this region could be used to test the results reported here. The modeling could be extended to older and younger sequences. The technique needs to be applied to an equally well determined Oligocene data set from another part of the world. Other eustatic proxies, such as $\delta^{18}O$ from the deep-sea record, could be compared to the two-dimensional sequence stratigraphic model results.

ACKNOWLEDGMENTS

This research was supported by National Science Foundation (NSF) grants EAR-95-06572, EAR-98-14025, and HRD-96-26177 to Kominz and EAR-94-17108 and EAR-97-08664 to K. Miller, and by the New Jersey Geological Survey. Cores were obtained by the New Jersey Coastal Plain Drilling Project (Ocean Drilling Program Legs 150X and 174AX), supported by the NSF Continental Dynamics and Ocean Drilling Programs and the New Jersey Geological Survey. We thank the Ocean Drilling Program for samples; K. Miller for discussions; and P. Heller, B. Wilkinson, and C. Kendell for insightful reviews.

REFERENCES CITED

Austin, J.A., Christie-Blick, N., Malone, M.J., et al., 1998, Initial reports, Ocean Drilling Program, Leg 174A: College Station, Texas, Ocean Drilling Program, 324 p.

Bandy, O.L., 1953, Ecology and paleoecology of some California foraminifera; Part I, The frequency distribution of recent foraminifera off California: Journal of Paleontology, v. 22, p. 161–182.

Berggren, W.A., Kent, D.V., Swisher, C.C., and Aubry, M.P., 1995, A revised Cenozoic geochronology and chronostratigraphy, *in* Berggren, W.A., et al., eds., Geochronology, time scales and global stratigraphic correlations: A unified temporal framework for an historical geology: SEPM (Society for Sedimentary Geology) Special Publication 54, p. 131–212.

Bond, G.C., 1979, Evidence for late Tertiary uplift of Africa relative to North America, South America, Australia, and Europe: Journal of Geology, v. 86, p. 47–65.

Bond, G.C., and Kominz, M.A., 1984, Construction of tectonic subsidence curves for the early Paleozoic miogeocline, southern Canadian Rocky Mountains: Implications for subsidence mechanisms, age of breakup, and crustal thinning: Geological Society of America Bulletin, v. 95, p. 155–173.

Bond, G.C., Kominz, M.A., Steckler, M.S., and Grotzinger, J.P., 1989, Role of thermal subsidence, flexure and eustasy in the evolution of early Paleozoic passive-margin carbonate platforms, *in* Crevello, P.D., et al., eds., Controls on carbonate platform and basin development: Society of Economic Paleontologists and Mineralogists Special Publication 44, p. 39–61.

Browning, J.V., Miller, K.G., and Bybell, L.M., 1997, Upper Eocene sequence stratigraphy and the Abscon Inlet Formation, New Jersey Coastal Plain, *in* Miller, K.G., and Snyder, S.W., Scientific results of the Ocean Drilling Program, Volume 150X: College Station, Texas, Ocean Drilling Program, p. 243–266.

Christie-Blick, N., 1991, Onlap, offlap, and the origin of unconformity-bounded depositional sequences: Marine Geology, v. 97, p. 35–56.

Christie-Blick, N., and Driscoll, N.W., 1995, Sequence stratigraphy: Annual Review of Earth and Planetary Science, v. 23, p. 451–478.

Cloetingh, S., 1986, Intraplate stresses: A new tectonic mechanism for fluctuations of relative sea level: Geology, v. 14, p. 617–620.

Fulthorpe, C.S., and Austin, J.A., Jr., 1998, The anatomy of rapid margin progradation: Three-dimensional geometries of Miocene clinoforms, New Jersey margin: American Association of Petroleum Geologists Bulletin, v. 82, p. 251–273.

Greenlee, S.M., and Moore, T.C., 1988, Recognition and interpretation of depositional sequences and calculation of sea-level changes from stratigraphic data—Offshore New Jersey and Alabama Tertiary, *in* Wilgus, C.K., et al., eds., Sea-level changes: An integrated approach: Society of Economic Paleontologists and Mineralogists Special Publication 42, p. 329–353.

Grow, J.A., Klitgord, K.D., Schlee, J.S., and Sheridan, R.E., 1988, Structure and evolution of Baltimore Canyon trough, *in* Sheridan, R.E., and Grow, J.A., eds., The Atlantic continental margin, U.S.: Boulder, Colorado, Geological Society of America, Geology of North America, v. I-2, p. 269–290.

Haq, B.U., Hardenbol, J., and Vail, P.R., 1987, Chronology of fluctuating sea levels since the Triassic (250 million years ago to present): Science, v. 235, p. 1156–1167.

Harrison, C.G.A., III, 1990, Long term eustasy and epeirogeny in continents, *in* Revelle, R., ed., Sea-level change: Washington, D.C., National Academy of Sciences, p. 141–158.

Heller, P.L., Wentworth, C.M., and Poag, C.W., 1982, Episodic post-rift subsidence of the United States Atlantic continental margin: Geological Society of America Bulletin, v. 93, p. 379–390.

Kafescioglu, I.A., 1975, A quantitative distribution of Foraminifera on the continental shelf and uppermost slope off Massachusetts: Micropaleontology, v. 21, p. 261–305.

Kominz, M.A., 1984, Oceanic ridge volumes and sea level change—An error analysis, *in* Schlee, J., ed., Interregional unconformities and hydrocarbon accumulation: American Association of Petroleum Geologists Memoir 36, p. 109–127.

Kominz, M.A., Miller, K.G., and Browning, J.V., 1998, Long-term and short term global Cenozoic sea-level estimates: Geology, v. 26, p. 311–314.

Lipps, J.H., Berger, W.H., Buzas, M.A., Douglas, R.G., and Ross, C.A., 1979, Foraminiferal ecology and paleoecology: Society of Economic Paleontologists and Mineralogists Short Course 6, 198 p.

Lithgow-Bertelloni, C., and Gurnis, M., 1997, Cenozoic subsidence and uplift of continents from time-varying dynamic topography: Geology, v. 25, p. 735–738.

Miller, K.G., and Fairbanks, R.G., 1985a, Cainozoic $\delta^{18}O$ record of climate and sea level: South African Journal of Sciences, v. 81, p. 248–249.

Miller, K.G., and Fairbanks, R.G., 1985b, Oligocene to Miocene carbon Isotope cycles and abyssal circulation changes, *in* Sundquist, E., and Broecker, W.S., eds.: The Carbon cycle and Atmospheric CO2: Natural var-

iation Archean to Present, Geography Monograph Ser., AGU, v. 32, p. 469–486.
Miller, K.G., Fairbanks, R.G., and Mountain, G.S., 1987, Tertiary oxygen isotope synthesis, sea-level history, and continental margin erosion: Paleoceanography, v. 2, p. 1–19.
Miller, K.G., Wright, J.D., and Fairbanks, R.G., 1991, Unlocking the ice house: Oligocene-Miocene oxygen isotopes, eustasy, and margin erosion: Journal of Geophysical Research, v. 96, p. 6829–6848.
Miller, K.G., Mountain, G.S., Blum, P., Gartner, S., Alm, P.-G., Aubry, M.-P., Burckle, L.H., Guerin, G., Katz, M.E., Christensen, B.A., Compton, J., Damuth, J.E., Deconinck, J.F., de Verteuil, L., Fulthorpe, C.S., Hesselbo, S.P., Hoppie, B.W., Kotake, N., Lorenzo, J.M., McCracken, S., McHugh, C.M., Quayle, W.C., Saito, Y., Snyder, S.W., ten Kate, W.G., Urbat, M., Van Fossen, M.C., Vecsei, A., Sugarman, P.J., Mullikin, L., Pekar, S., Browning, J.V., Liu, C., Feigenson, M.D., Goss, M., Gwynn, D., Queen, D.G., Powars, D.S., Heibel, T.D., Bukry, D., 1996, Drilling and dating New Jersey Oligocene-Miocene sequences: Ice volume, global sea level, and Exxon records: Science, v. 271, p. 1092–1095.
Miller, K.G., Browning, J.V., Pekar, S.F., and Sugarman, P.J., 1997, Cenozoic evolution of the New Jersey Coastal Plain: Changes in sea level, tectonics, and sediment supply, *in* Miller, K.G., and Snyder, S.W., Scientific results of the Ocean Drilling Program, Volume 150X: College Station, Texas, Ocean Drilling Program, p 361–373.
Miller, K.G., and Sugarman, P.J., et al., 1998a, Bass River Site Report: Initial reports, New Jersey Coastal Plain, Ocean Drilling Program, Leg 174AX: College Station, Texas, Ocean Drilling Program, 43 p.
Miller, K.G., Mountain, G.S., Browning, J.V., Kominz, M.A., Sugarman, P.J., Christie-Blick, N., Katz, M.E., and Wright, J.D., 1998b, Cenozoic global sea-level, sequences, and the New Jersey Transect: Results from coastal plain and slope drilling: Reviews of Geophysics, v. 36, p. 569–601.
Monteverde, D.H., Miller, K.G., and Mountain, G.S., 2000, Correlation of offshore seismic profile with onshore New Jersey Miocene sediments: Sedimentary Geology, v. 134, p. 111–127.
Murray, J.W., 1973, Distribution and ecology of living benthic foraminiferids: New York, Crane, Russak and Co., 274 p.
Nyong, E.O., and Olsson, R.K., 1984, A paleo-slope model of Campanian to lower Maestrichtian foraminifera in the North American basin and adjacent continental margin: Marine Micropaleontology, v. 8, p. 437–477.
Olsson, R.K., 1991, Cretaceous to Eocene sea-level fluctuations on the New Jersey margin: Sedimentary Geology, v. 70, p. 195–208.
Olsson, R.K., Miller, K.G., and Ungrady, T.E., 1980, Late Oligocene transgression of the middle Atlantic coastal plain: Geology, v. 8, p. 549–554.
Pekar, S.F., 1999, A new method for extracting water depth, relative sea-level, and eustatic records from onshore New Jersey Oligocene sequence stratigraphy [Ph.D. dissert.]: Piscataway, New Jersey, Rutgers University, 187 p.
Pekar, S.F., and Kominz, M.A., 2001, Benthic foraminiferal biofacies water depth estimates from the onshore New Jersey Oligocene strata using a two-dimensional paleoslope model: Journal of Sedimentary Research.
Pekar, S.F., and Miller, K.G., 1996, New Jersey Oligocene ''Icehouse'' sequences (ODP Leg 150X) correlated with global $\delta^{18}O$ and Exxon eustatic records: Geology, v. 24, p. 567–570.
Pekar, S.F., Miller, K.G., and Browning, J.V., 1997, New Jersey coastal plain Oligocene sequences, *in* Miller, K.G., and Snyder, S.W., eds., Scientific results of the Ocean Drilling Program, Volume 150X: College Station, Texas, Ocean Drilling Program, p. 187–206.
Pekar, S.F., Miller, K.G., and Kominz, M.A., 2000, Reconstructing the stratal geometry of latest Eocene to Oligocene sequences: New Jersey, Resolving a patchwork distribution into a clear pattern of progradation: Sedimentary Geology, v. 134, p. 93–109.
Phleger, F.B., and Parker, F.L., 1951, Ecology of foraminifera, northwest Gulf of Mexico, Part II, Foraminifera species: Geological Society of America Memoir 46, p. 1–64.
Pinous, O.V., Akhmetiev, M.A., and Sahagian, D.L., 1999, Sequence stratigraphy and sea-level history of Oligocene strata of the northern Aral Sea region (Kazakhstan): Implications for glacioeustatic reconstructions: Geological Society of America Bulletin, v. 111, p. 1–10.
Poore, R.Z., and Bybell, L.M., 1988, Eocene to Miocene biostratigraphy of New Jersey Core ACGS #4: Implications for regional stratigraphy: U.S. Geological Survey Bulletin 1829, p. 1–22.
Posamentier, H.W., and Vail, P.R., 1988, Eustatic controls on clastic deposition II—Sequence and systems tract models, *in* Wilgus, C.K., et al., eds., Sea-level changes: An integrated approach: Society of Economic Paleontologists and Mineralogist Special Publication 42, p. 109–123.
Poulsen, C.J., Flemings, P.B., Robinson, R.A.J., and Metzger, J.M., 1998, Three-dimensional stratigraphic evolution of the Miocene Baltimore Canyon region: Implications for eustatic interpretations and the systems tract model: Geological Society of America Bulletin, v. 110, p. 1105–1122.
Reynolds, D.J., Steckler, M.S., and Coakley, B.J., 1991, The role of the sediment load in sequence stratigraphy: The influence of flexural isostasy and compaction: Journal of Geophysical Research, v. 96, p. 6931–6949.
Rhodehamel, E.C., 1977, Sandstone porosities, *in* Scholle, P.A., ed., Geological studies on the COST no. B-2 well, U.S. mid-Atlantic outer continental shelf area: U.S. Geological Survey Circular 750, p. 23–31.
Sahagian, D.L., 1988, Ocean temperature-induced change in lithospheric thermal structure: A mechanism for long-term eustatic sea level change: Journal of Geology, v. 96, p. 254–261.
Sahagian, D.L., and Jones, M., 1993, Quantified Middle Jurassic through Paleogene eustatic variations based on Russian platform stratigraphy: Stage-level resolution: Geological Society of America Bulletin, v. 105, p. 1109–1118.
Schlanger, S.O., Jenkyns, H.C., and Premoli-Silva, I., 1981, Volcanism and vertical tectonics in the Pacific Basin related to global Cretaceous transgressions: Earth and Planetary Science Letters, v. 52, p. 435–449.
Schnitker, D., 1970, Upper Miocene foraminifera from near Grimeland, Pitt County, North Carolina: Raleigh, North Carolina Department of Conservation and Development, 129 p.
Schnitker, D., 1971, Distribution of Foraminifera on the North Carolina continental shelf: Tulane Studies in Geology and Paleontology, v. 8, p. 169–215.
Sen Gupta, B.K., 1971, The benthonic foraminifera of the tail of the Grand Banks: Micropaleontology, v. 17, p. 69–98.
Smith, M.A., Amato, R.V., Furbush, M.A., Pert, D.M., Nelson, M.E., Hendrix, J.S., Tamm, L.C., Wood, G., Jr., and Shaw, D.R., 1976, Geological and operational summary, COST no. B-2 well, Baltimore Canyon Trough area, Mid-Atlantic OCS: U.S. Geological Survey Open-File Report 76–774, 79 p.
Steckler, M.S., Watts, A.B., and Thorne, J.A., 1988, Subsidence and basin modeling at the U.S. Atlantic passive margin, *in* Sheridan, R.E., and Grow, J.A., eds., The Atlantic continental margin: U.S.: Boulder, Colorado, Geological Society of America, Geology of North America, v. I-2, p. 399–416.
Steckler, M.S., Mountain, G.S., Miller, K.G., and Christie-Blick, N., 1999, Reconstruction of Tertiary progradation and clinoform development on the New Jersey passive margin by 2-D backstripping: Marine Geology, v. 154, p. 399–420.
Vail, P.R., and Mitchum, R.M., Jr., 1977, Seismic stratigraphy and global changes of sea-level, Part 1: Overview, *in* Payton, C.E., ed., Seismic stratigraphy—Applications to hydrocarbon exploration: American Association of Petroleum Geologists Memoir 26, p. 51–52.
Walton, W.R., 1964, Recent foraminiferal ecology and paleoecology, *in* Imbrie, J., and Newell, N., eds., Approaches to paleoecology: New York, John Wiley, p. 151–237.
Watts, A.B., and Steckler, M.S., 1979, Subsidence and eustasy at the continental margin of eastern North America, *in* Talwani, M., et al., eds., Deep drilling results in the Atlantic Ocean; continental margins and paleoenvironment: American Geophysical Union Maurice Ewing Series 3, p. 218–234.
Zachos, J.C., Breza, J., and Wise, S.W., 1992a, Earliest Oligocene ice-sheet expansion on East Antarctica: Stable isotope and sedimentological data from Kerguelen Plateau: Geology, v. 20, p. 569–573.
Zachos, J.C., Rea, D.K., Seto, K., Niitsuma, N., and Nomura, R., 1992b, Paleogene and early Neogene deep water history of the Indian Ocean: inferences from stable isotopic records, *in* Duncan, R.A., et al., eds., The Indian Ocean: A synthesis of results from the Ocean Drilling Program: American Geophysical Union Geophysical Monograph 70, p. 351–386.

MANUSCRIPT RECEIVED BY THE SOCIETY MAY 27, 1999
REVISED MANUSCRIPT RECEIVED DECEMBER 20, 1999
MANUSCRIPT ACCEPTED FEBRUARY 28, 2000

Printed in the USA